

## Design of Y-Type Branch Broadband Dual-polarization Antenna and C-Type Slot Line Notch Antenna

Yan Yan, Lan Li, Jifang Zhang, Heming Hu, Yonghao Zhu, Hua Chen\*, and Qing Fang

**Abstract**—In order to satisfy the requirements of 2G/3G/4G wireless communication, two kinds of base station antennas with wideband, dual-polarized and three-modes are proposed in this paper. Firstly, a pair of diamond dipoles is placed in an orthogonal way to realize dual-polarizations, then a pair of Y-shaped branches is added to generate a new mode. The Y-type coupling feeding can increase the impedance bandwidth without increasing the size of antenna. The antenna achieves an impedance bandwidth of 51.75% (1.69–2.87 GHz) with a return loss lower than  $-14$  dB. The antenna also has a stable radiation performance. The gain is greater than 8.6 dBi, and the port isolation is less than  $-27$  dB over the entire frequency band. Then based on above antenna, a C-type slot notched antenna is added to improve anti-interference ability. Finally, band stop characteristics are obtained by etching a C-type slot line resonator on two dipoles. The results show that the bandwidth is 1.7–2.69 GHz, and the sharp notched band is 1.8–1.95 GHz. The C-type slot line here can be regarded as a quarter wavelength resonator in series. Moreover, the isolation of the port is less than  $-28$  dB, and the 3 dB beamwidth in the bandwidth is  $66 \pm 5^\circ$ . Both antennas are fabricated and have dual polarizations, simple structure, and good radiation performance, which can be used in the next generation of wireless communication.

### 1. INTRODUCTION

With the rapid development of wireless communication technology [1], dual-polarized antennas have been widely used in base stations for mobile communication. As a vital component of base-station systems, antennas must satisfy many requirements, such as wide impedance bandwidth, stable gain, miniaturization, stable radiation pattern, low cross polarization radiation, and dual polarized performance [2]. Among them, cross dipole has the advantage of broadband. Therefore, plenty of cross dipoles have been proposed, and many of them have a double-modes characteristic [3–7]. At present, the most effective way to enhance bandwidth is to introduce new resonance points which is multi-mode formation bandwidth. By embedding additional cross-loops in the original cross-loops [8], the additional cross-loops would form new resonance points at high frequencies to increase the antenna bandwidth without increasing the size of antenna. A broadband antenna with Y-shaped feeding is presented in [9]. Compared to the traditional direct feed, the antenna achieves a 45% impedance bandwidth for  $VSWR < 1.5$ , a stable radiation pattern, and a stable gain.

Before the base station antenna satisfies the broadband requirements, the transmitting antenna and receiving antenna will interfere with each other in the array. Although a multi-frequency antenna can be designed to solve this problem, it will increase the number of antennas, resulting in the tension of station location. If the interference frequency band can be filtered directly from the broadband antenna, this problem can be solved well. In microstrip antenna, broadband microstrip filter antenna has made great progress. However, in base station antenna, the antenna with filter structure rarely appears. In [10–12], the filtering is realized by etching L-shaped, U-shaped, and C-shaped slots on the

---

*Received 25 October 2021, Accepted 1 December 2021, Scheduled 15 December 2021*

\* Corresponding author: Hua Chen (cherrychen40600@163.com).

The authors are with the Faculty of Science, Kunming University of Science and Technology, Kun Ming 650093, China.

radiation structure. In [13], a Circular Complementary Split Ring Resonator (CSRR) is introduced as a band stop structure on the circular radiation patch of the antenna, and the notch function at the response frequency point is also realized. In [14], the periodic electromagnetic band gap structure element is placed in the symmetrical position on both sides of the microstrip feed line of the Ultra Wide Band (UWB) antenna, and the antenna also obtains a better notch frequency band. In order to obtain sharp band stop response in the required notch frequency band, two or three resonators with the same resonant frequency are used in appropriate positions in [15] and [16]. The flexible band notch of a broadband long-term evolution (LTE) base station antenna introduces two window slots to etch on the radiation patch of the magnetoelectric dipole [17], but the size of the antenna is too large for the use of the antenna array. In [18], in the frequency band of 1.65–2.9 GHz, the notch frequency band of 2.27–2.53 GHz is realized by arranging the C-shaped stub beside the feeder. In [19], a broadband dual polarization filter dipole antenna for base station is introduced. By adding two parasitic loops on the line, a filter base station antenna with band-pass characteristics is realized.

In this paper, we propose a novel broadband dual polarized antenna for 2G/3G/4G wireless communication. The antenna has a wide impedance bandwidth, a stable radiation pattern, and a stable gain simultaneously. By introducing new branches, the antenna obtains new resonance points and increases bandwidth without increasing the size of antenna. It achieves a bandwidth of 51.75% (1.69–2.87 GHz) for VSWR < 1.5 and isolation between ports less than –26 dB. Based on the structure of Fig. 1, a dual-polarization base station antenna with good selectivity is designed. Without introducing additional structure, the designed antenna realized band stop notch antenna by etching a C-type slot line in DCS1800 frequency band. The coverage frequency range is 1.7–2.69 GHz, and it has better return loss (VSW < 1.5) in the required frequency range. The antenna forms a peak of band resistance on band 1.8–1.95 GHz. The isolation between ports is less than –28 dB. Both antennas are designed with printed circuit board (PCB), which have the advantages of low production cost and convenience processing.

## 2. WIDEBAND ANTENNA WITH Y-SHAPED BRANCH

### 2.1. Antenna Structure

As shown in Fig. 1, the antenna consists of two pairs of cross diamond dipoles, two Y-shaped feeding structures, and a box reflector. Two pairs of diamond dipoles and Y-shaped branches are printed on the back of an FR4 substrate with a thickness of  $H_0 = 1$  mm, dielectric permittivity of 4.4, and loss tangent of 0.02. Y-type coupling feeding microstrip lines are printed on the top of the FR4. The inner conductors of two 50  $\Omega$  coaxial cables are connected to the feeding microstrip lines. The outer conductors of the 50  $\Omega$  coaxial cables are connected to the diamond dipoles. In order to prevent the two pairs of microstrip lines from crossing each other, a pair of microstrip lines is specially treated. The dipole is placed on a square reflector box with a height of  $\lambda_0/2 = 34$  mm, where the wavelength of  $\lambda_0$  is corresponding to the center frequency 2.2 GHz in free space.

Since the diamond dipole cannot satisfy the broadband 1.7–2.7 GHz, we introduce a new resonant point to extend the frequency band. The new resonance point can be controlled by Y-shaped branches separately, which result in the new resonance point close to the second resonance point to form a bandwidth.

### 2.2. Operating Principle

In order to introduce a new resonant point more intuitively, we compare the impedance changes of the diamond dipole with the diamond dipole with Y-shaped branches. It can be seen from Fig. 2 that the resistance near the high frequency of 2.7 GHz by the loading of the Y-shaped branch is maintained at about 50  $\Omega$ . In order to further improve the impedance bandwidth, the Y-branch is added. By increasing the length of Y-shaped branch F11, we find that new resonance points appear at high frequencies with the increase of length. When this resonance point approaches the second resonance point, a broadband is formed. The appearance of this resonance point does not affect the first two resonance points, which can be controlled separately.

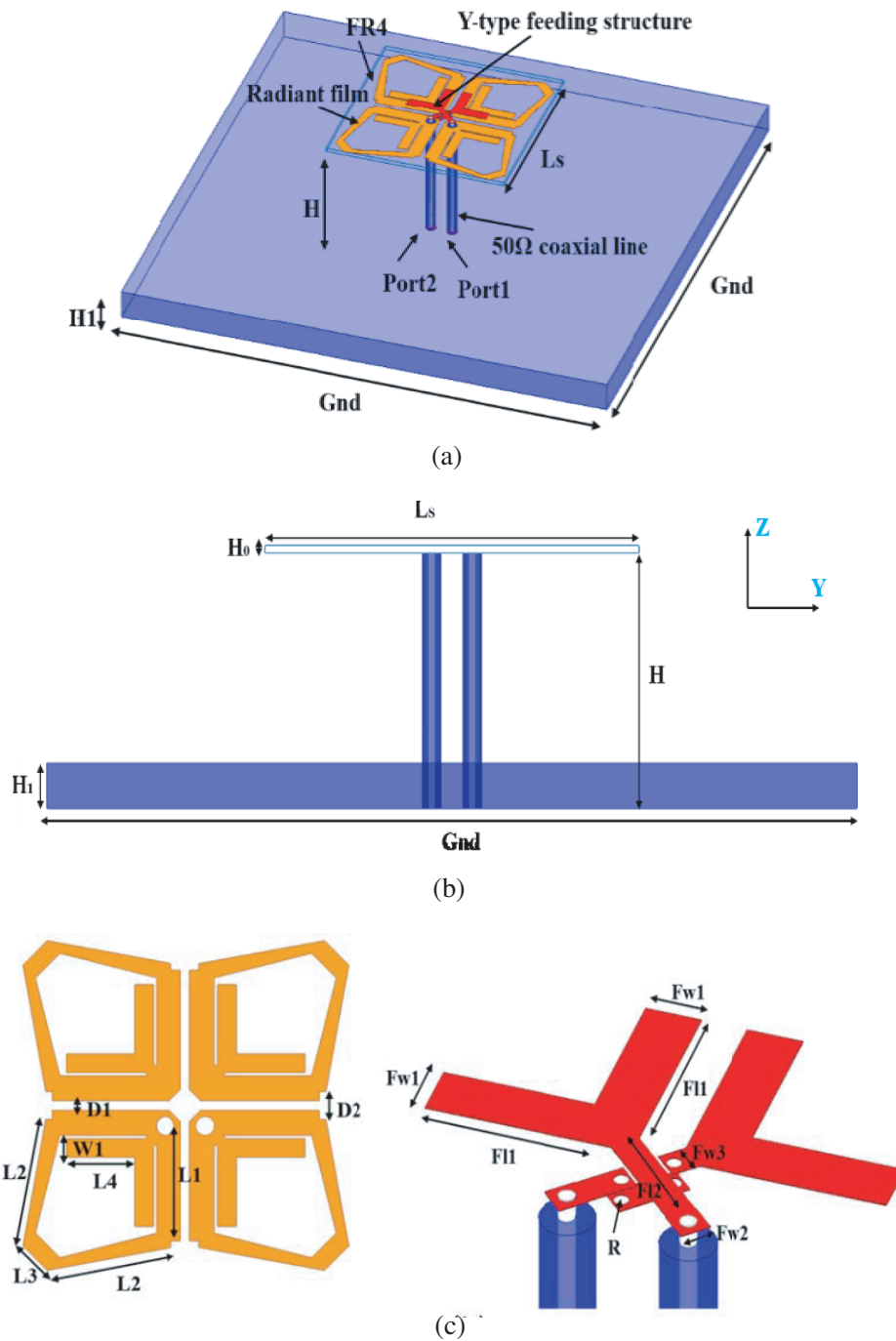


**Figure 1.** (a) Antenna geometry; (b) Antenna side view; (c) Radiation element structure and feeding structure.

This can be explained by examining the current distribution on the dual polarized antenna elements. As shown in Fig. 3, the  $+45^\circ$  polarized dipole is excited with or without a Y-shaped branch. It is found that the current distribution above the Y-shaped branch was opposite to the current distribution of the diamond dipole. At 1.7 GHz, the main current on the diamond dipole is much larger than the opposite current on the Y-branch. Therefore, the total current path of the dipole hardly changes. At higher frequencies of 2.7 GHz, the reverse current of the branches is stronger. The other polarization ( $-45^\circ$ ) acts as a parasitic element in terms of current distribution and does not participate in radiation. As

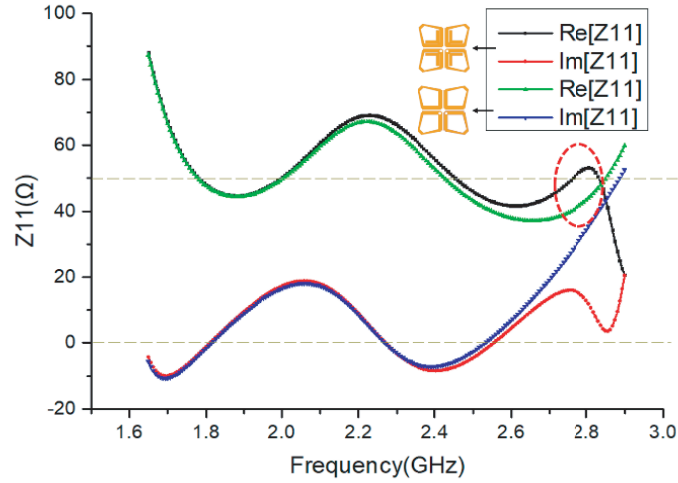


**Figure 2.**  $Z$ -parameter of antenna with or without Y-branch ( $Z_{11}$ ).

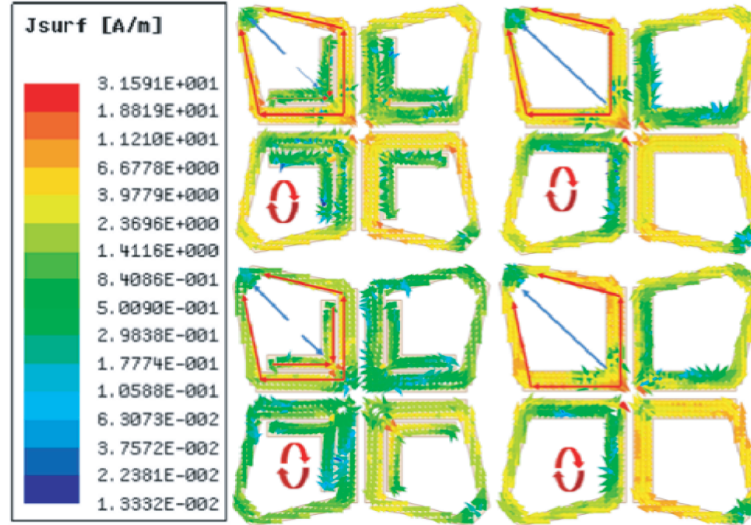


**Figure 3.** Broadband dual-polarized current distribution in the presence or absence of Y-shaped branches at frequencies of 1.7 GHz and 2.7 GHz.

a result, since the reverse current and the main current cancel, the total current path becomes short. It is well known that the radiation resistance of a dipole is proportional to the electrical length of the current path [20].

In summary, due to the existence of the Y-shaped branch, the impedance bandwidth of the modified antenna is widened. The current length of a resonant mode is equal to  $2 \times L1 + 2 \times L2 + L3 \approx 0.57\lambda_1$ , where  $\lambda_1$  is the free-space wavelength at the first resonant frequency (1.8 GHz). Due to the strong coupling between the dipoles,  $L1$ ,  $D1$  and  $D2$  have a large effect on the second resonant frequency. The third resonant frequency is primarily determined by the size of  $L4$  and  $W1$ , and the circuit path length is approximately equal to  $2 \times L4 \times \sqrt{2} \approx 0.4\lambda_2$ , where  $\lambda_2$  is the free-space wavelength at the third resonant frequency (2.82 GHz).

For understanding the influence of the Y-shaped branch on the antenna, we performed the parameter sweeping by taking the length  $L4$  of the branch. The antenna model was scanned and optimized using the software HFSS 20.0. It can be seen from Fig. 4 that as the length of  $L4$  increases, a new resonance point appears at a high frequency and is constantly approaching the second resonance

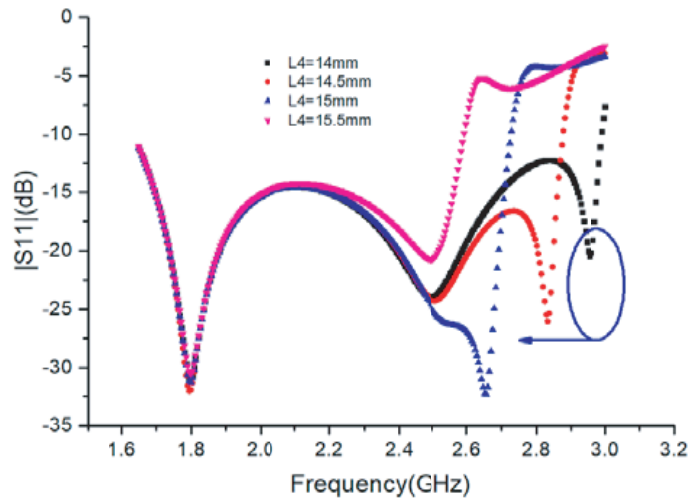


**Figure 4.** Effect of the length ( $L4$ ) on  $S_{11}$  of the proposed antenna.

point. When the length  $L4$  of the branch is 14.5 mm, the impedance bandwidth is formed with the second resonance point of the original antenna, so that the antenna has a VSWR  $> 1.5$  in the frequency range of 1.69 to 2.87 GHz. The antenna covers the 2G/3G/4G bands and has a wider impedance bandwidth. The final optimization values of this paper are as follows (unit: mm):  $L1 = 18.97$ ,  $L2 = 20.42$ ,  $L3 = 5.55$ ,  $L4 = 14.5$ ,  $D1 = 0.75$ ,  $D2 = 4.46$ ,  $W1 = 3$ ,  $Fw1 = 9.66$ ,  $Fw1 = 3$ ,  $Fw2 = 1.7$ ,  $Fw2 = 6.25$ ,  $Fw3 = 1.6$ ,  $R = 0.4$ ,  $Ls = 55$ ,  $H = 34$ ,  $H1 = 6$ ,  $Gnd = 140$ .

### 2.3. Results

For validation, a prototype of the proposed Y-type branch broadband dual-polarization antenna was fabricated and tested. Fig. 5 shows the fabricated prototype of the antenna. To verify the design, we use AV3656A vector network analyzer which is produced by CETC (China Electronics Technology Group Corporation) for antenna measurement. The simulated and measured  $S$ -parameters of the designed dual-polarized antennas are shown in Fig. 6. The results show that at port 1 and port 2, the antenna achieves the magnitude of  $S_{11}$  lower than  $-14$  dB and  $S_{21}$  lower than  $-27$  dB in the range of 1.69–

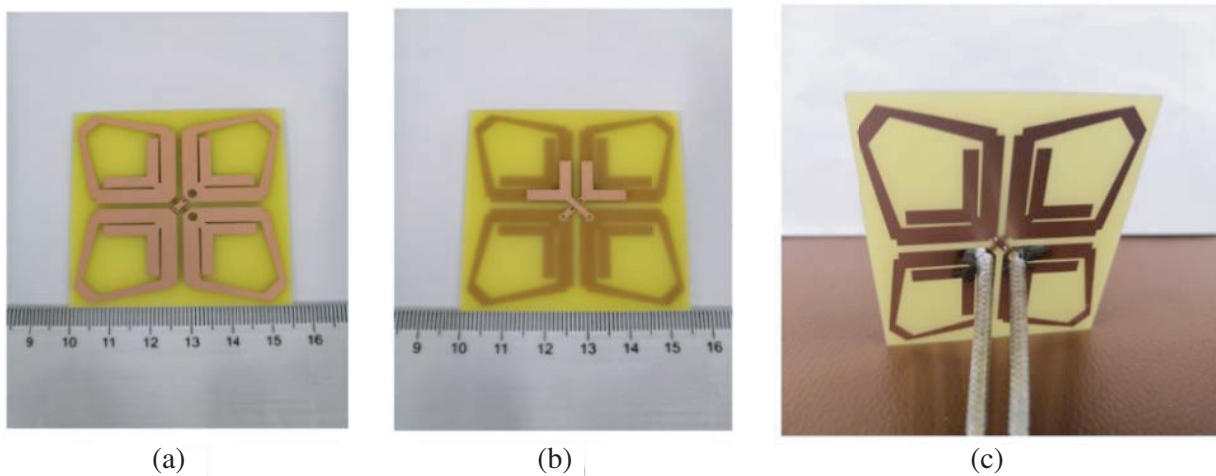


**Figure 5.** Prototype of the proposed Y-type branch broadband dual-polarization antenna. (a) Top view of the prototype. (b) Bottom view of the prototype. (c) Perspective view of the prototype.

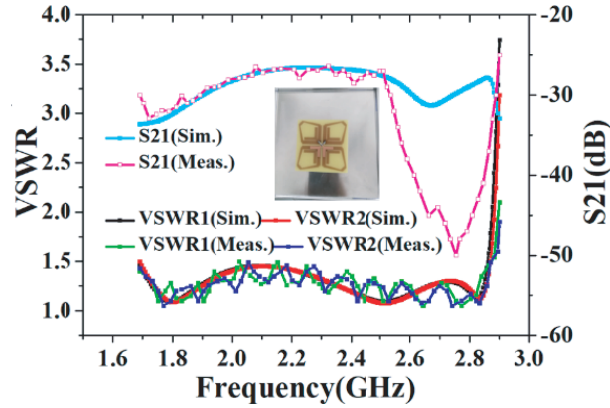


**Figure 6.** Simulated and measured *S*-parameters of dual-polarized antennas.

2.87 GHz. This means that the port has good return loss and isolation performance, and the two ports are highly consistent.

When port 1 is energized, Fig. 7 shows the normalized radiation pattern of the antenna in horizontal plane. These include primary polarization and cross polarization, labeled ‘co-pol’ and ‘x-pol’, respectively. The measured results show that the antenna has a half-power beamwidth of  $65 \pm 5^\circ$  and  $\pm 60^\circ$ , and the cross-polarization ratio is better than 9 dBi at frequencies of 1.7 GHz, 2.2 GHz, and 2.7 GHz. The measured and simulated results are in good agreement. The antenna has a stable pattern and a good cross polarization ratio. Due to the highly symmetrical antenna structure, only the radiation pattern of port 1 is given.

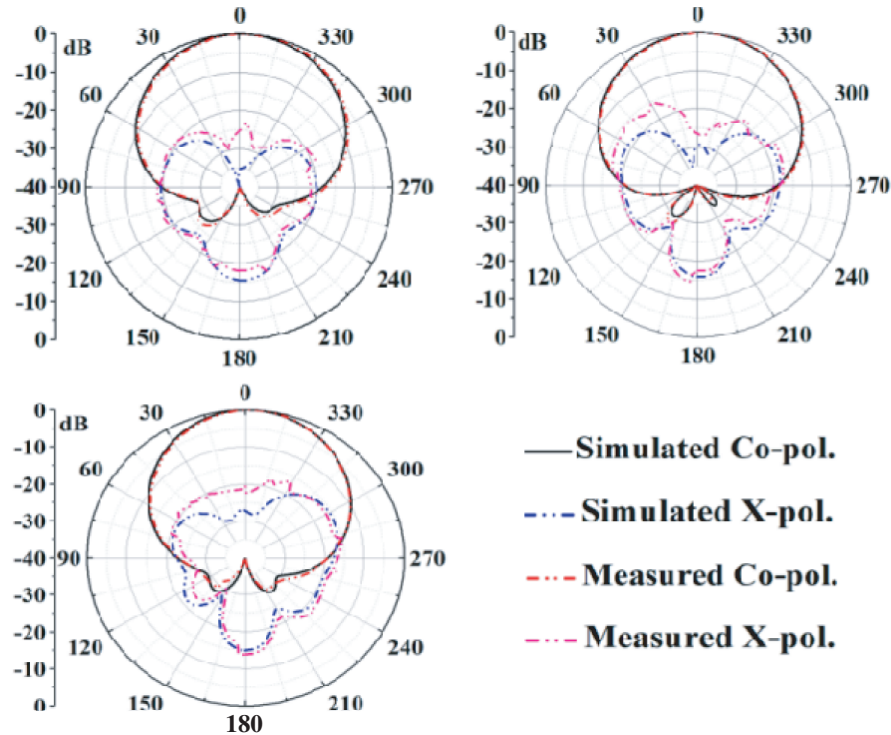


**Figure 7.** Radiation patterns of antennas at frequencies of 1.7 GHz, 2.2 GHz and 2.7 GHz.

### 3. NOTCHED ANTENNA STRUCTURE

#### 3.1. Antenna Structure

In this part, a dual polarization base station antenna with band resistance is proposed. Filtering out the interference of DCS1800 frequency band, the antenna working frequency band could cover all 2G/3G/4G bands. Each pair of dipoles adopts a C-type resonator. By using the resonant characteristics of C-type slot, the DCS1800 band is filtered out, and the selectivity of the antenna is improved. The size of the notch antenna is  $(60 \times 60 \times 34 \text{ mm}^3)$ , and it is designed with printed circuit board (PCB), which is easy to process and low in price.

The antenna structure is shown in Fig. 8. Two pairs of orthogonal dipoles are printed on the bottom layer of a dielectric substrate FR4, and the Y-type coupling feeding structure is printed on the top layer of the FR4. The basic dimensions of dipole and Y-type feeding in Fig. 8 are the same as those in Fig. 1, but some parameters are optimized. The antenna adopts a plane diamond dipole, which is different from Fig. 1 in that there is no hollowing out the middle part. To get better degrees of freedom, a plane dipole is used to design the space on the filter antenna. A pair of C-type resonant slots is opened on the diamond dipole to filter out the DCS1800 frequency band. In order to realize directional radiation, a reflective plate with flanging is added at the wavelength  $1/4$  below the antenna. The etched C type resonant slot line is (unit: mm):  $L4 = 6.55$ ,  $L5 = 11.5$ ,  $L6 = 15.5$ .

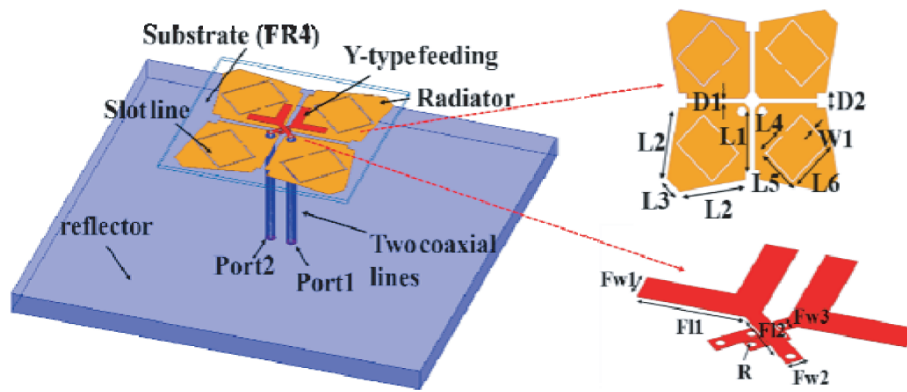


Figure 8. Antenna structure.

#### 3.2. Operating Principle

Firstly, a wideband miniaturized antenna based on a planar cross dipole is designed. The antenna consists of a pair of orthogonal planar diamond dipoles, a pair of Y-type coupling feeding, a pair of  $50 \Omega$  coaxial lines, and a reflector with flanging. The Y-type coupling feeding is used to adjust the impedance matching of the antenna. Secondly, in order to widen the working bandwidth of the antenna, the diamond dipole is chamfered. By changing the coupling strength between the dipoles,  $VSWR < 1.5$  in the range of 1.69–2.7 GHz is achieved. Thirdly, in order to filter out the interference of DCS1800 frequency band, a C-type slot line is etched on each pair of dipoles. The length of C-type slot line is  $2 \times (L4 + L5 + L6) \approx \lambda/4$ , where  $\lambda$  is the free space wavelength at the resonant frequency 1.85 GHz. It can be seen from Fig. 9 that a sharp band stop is formed in the frequency band of 1.8–1.95 GHz.

As shown in Fig. 10, the C-type slot line can be regarded as a quarter wavelength resonator in series. When the C-type slot resonates at the working frequency, the impedance at the end of the slit can be regarded as 0. After a quarter impedance transformation, the impedance at the middle of the C-shaped slit can be seen as infinite, which can be equivalent to an open circuit. Therefore, the energy cannot be radiated to the antenna unit effectively. Due to the stopband characteristic of the antenna changes according to the length of the C-type slot, the desired notch resonance point can be obtained by controlling the length of the C-type slot.

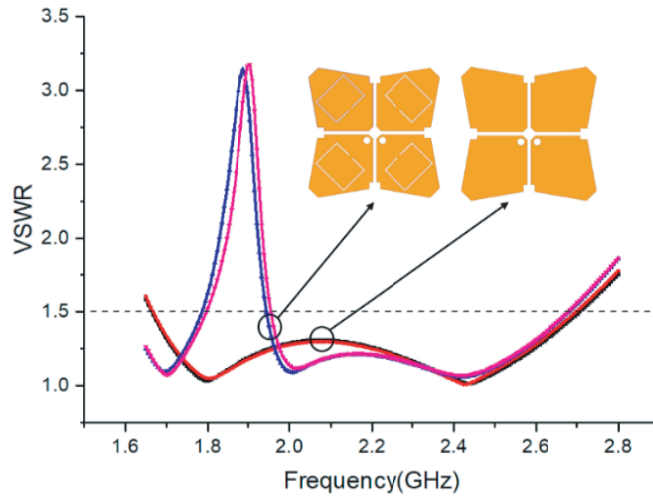


Figure 9. Return loss of antenna with or without resonant slot.

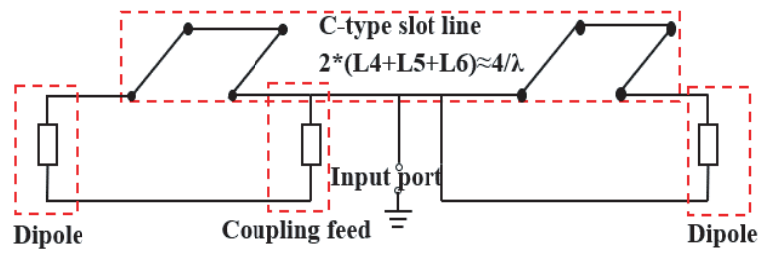


Figure 10. Equivalent circuit diagram of notch antenna.

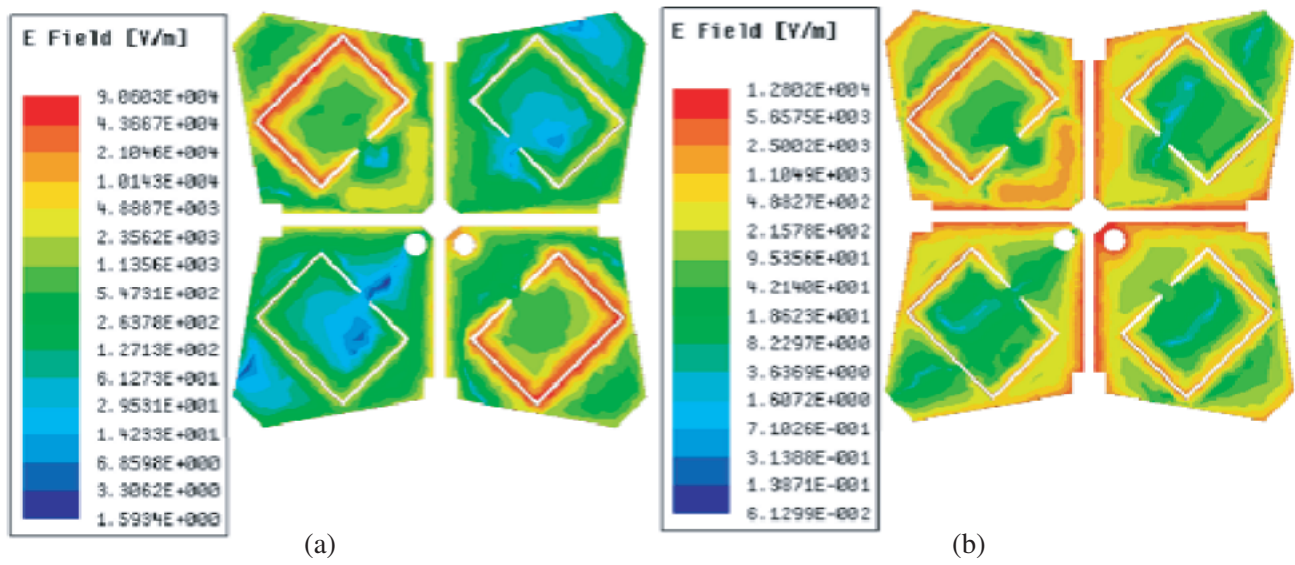


Figure 11. (a) Electric field distribution of antenna at 1.85 GHz; (b) Electric field distribution of antenna at 2.2 GHz.



In order to better understand the working principle of C-type slot line, the electric field distribution at the frequency points of 1.85 GHz and 2.2 GHz is analyzed. When the  $+45^\circ$  polarized port is excited, the energy of the 1.85 GHz  $+45^\circ$  dipole at the frequency point is mainly concentrated around the C-shaped slot, and no energy is radiated into the free space, shown in Fig. 11. When the frequency point is 2.2 GHz, although part of the energy is also gathered around the C-type slot line, it does not affect the electric field distribution in the main radiation direction of the antenna.

### 3.3. Results

A prototype of the proposed C-type slot line notch antenna is fabricated as shown in Fig. 12. HFSS 20.0 is used for simulation, and measured results are verified by AV3656A vector network analyzer. In Fig. 13, we can see that the return loss of the antenna with working bandwidth 1.7–2.69 GHz is less than  $-14$  dB ( $VSWR < 1.5$ ). The isolation between ports is better than 28 dB. The gain of the two ports is kept at  $8.6 \pm 0.5$  dBi. In the defect band, its gain is reduced to  $-2.1$  dBi and  $-1.7$  dBi, respectively as shown in Fig. 14. It can filter out the unnecessary DCS1800 band, and the antenna has good selectivity. The HBPW of the notch antenna is  $66 \pm 5^\circ$ . It has good main polarization and  $\pm 60^\circ$  cross polarization. In Fig. 15, the antenna has good far-field radiation at 1.7 GHz, 2.2 GHz, and 2.69 GHz.

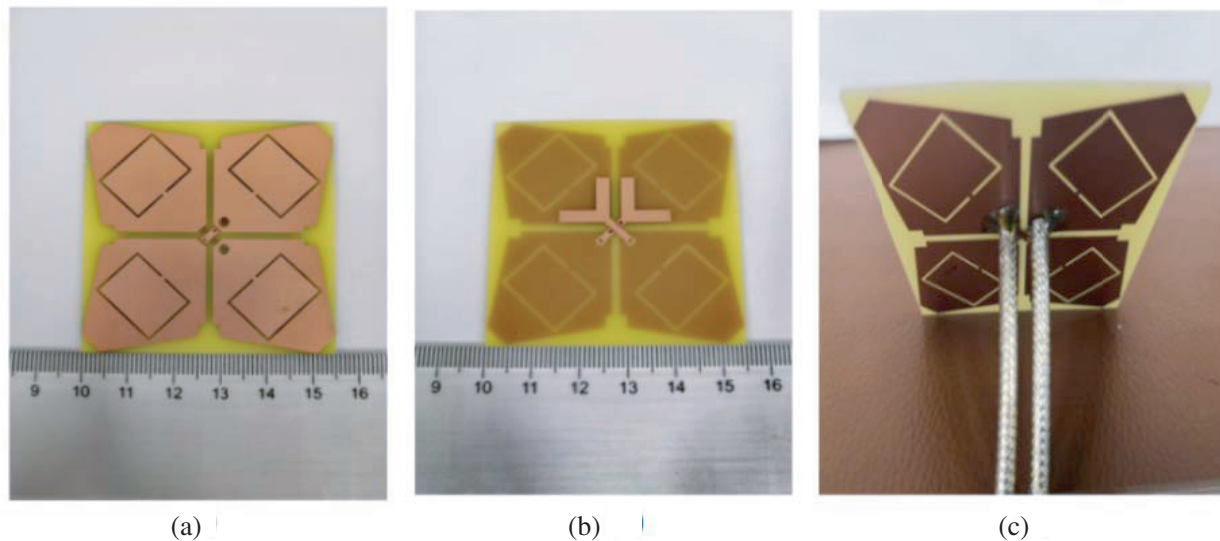


**Figure 12.** Prototype of the proposed C-type slot line notch antenna. (a) Top view of the prototype. (b) Bottom view of the prototype. (c) Perspective view of the prototype.

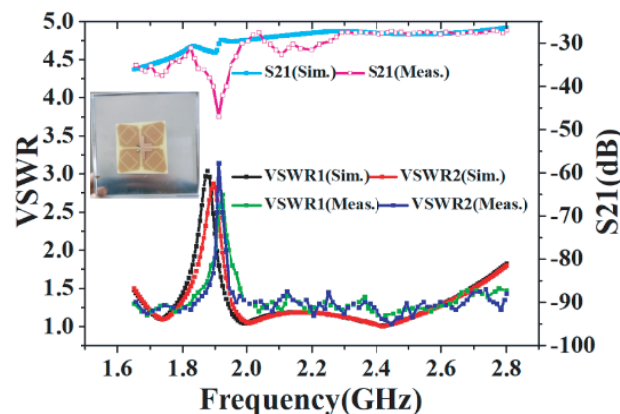


**Figure 13.** Simulated and measured  $S$  parameter of antenna.

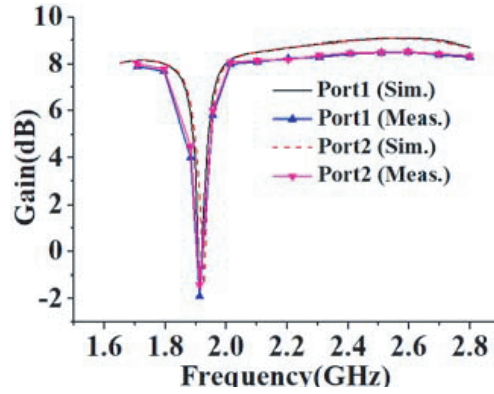


**Figure 14.** Simulated and measured gain of notch antenna.

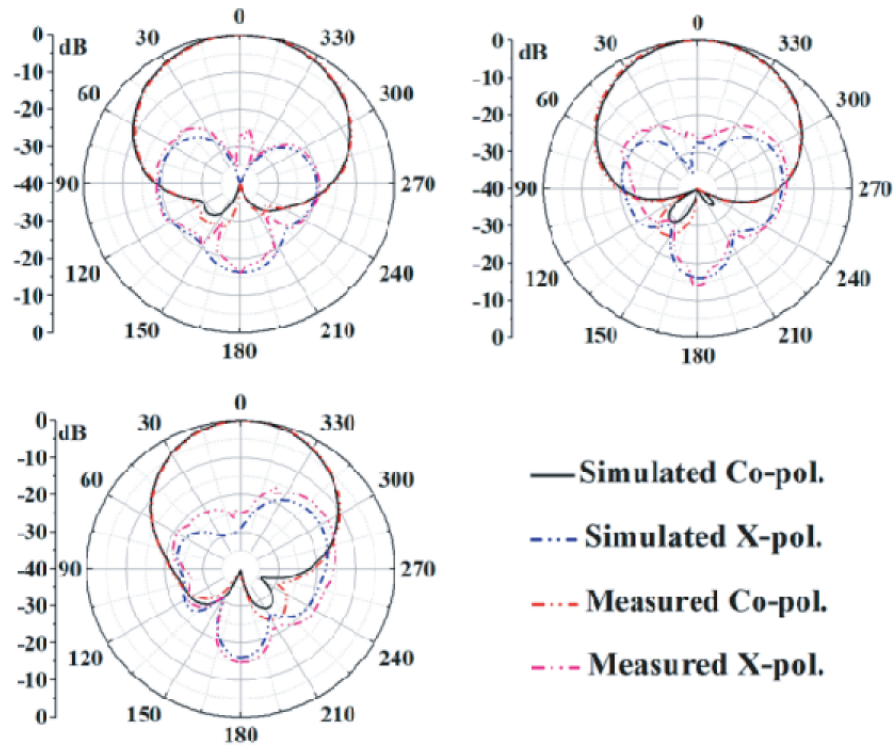


**Figure 15.** Simulated and measured radiation patterns of antennas at frequencies of 1.7 GHz, 2.2 GHz and 2.7 GHz.

#### 4. CONCLUSION

In this paper, two kinds of dipole base station antennas with dual polarizations, wideband, and three-modes are designed and fabricated. A pair of Y-shaped branches is employed to generate a new mode, then the band rejection characteristic can be obtained by adding a C-type slot notch. Finally, the designed antennas can cover 2G/3G/4G bands. The measured results show that the return loss of the antenna is less than  $-14$  dB, and the port isolation is lower than  $-27$  dB. The half-power beamwidth is  $65^\circ \pm 5^\circ$ , and the gain is around 9 dBi over the entire frequency range. The notch antenna can form a spike in the DCS1800 frequency band by etching a C-type resonant slot line in the dipole. The gain of the two polarizations can decrease to  $-2.1$  dBi and  $-1.7$  dBi, respectively. The results shown that the antennas have good circuit performance and radiation performance.

## ACKNOWLEDGMENT

The authors thank the support of National Key Research and Development Program of China (2018YFB2200500); National Natural Science Foundation of China (61764008).

## REFERENCES

1. Chen, Z. N. and K. M. Luk, *Antennas for Base Stations in Wireless Communications*, 1–10, The McGraw-Hill Companies, 2009.
2. Xue, Q., S. W. Liao, and J. H. Xu, “A differentially-driven dual-polarized magneto-electric dipole antenna,” *IEEE Trans. Antennas Propag.*, Vol. 61, No. 1, 425–430, Jan. 2013.
3. Su, D., J. J. Qian, H. Yang, and D. Fu, “A novel broadband polarization diversity antenna using a cross-pair of folded dipoles,” *IEEE Antennas Wireless Propag. Lett.*, Vol. 4, 433–435, 2005.
4. Liu, Y., H. Yi, F. W. Wang, and S. X. Gong, “A novel miniaturized broadband dual-polarized dipole antenna for base station,” *IEEE Antennas Wireless Propag. Lett.*, Vol. 12, 1335–1338, 2013.
5. Chu, Q. X. and Y. Luo, “A broadband unidirectional multi-dipole antenna with very stable beamwidth,” *IEEE Trans. Antennas Propag.*, Vol. 61, No. 5, 2847–2852, 2013.
6. Cui, Y., R. Li, and H. Fu, “A broadband dual-polarized planar antenna for 2G/3G/LTE base stations,” *IEEE Trans. Antennas Propag.*, Vol. 62, No. 9, 4836–4840, Sept. 2014.
7. Gou, Y., S. Yang, J. Li, and Z. Nie, “A compact dual-polarized printed dipole antenna with high isolation for wideband base station applications,” *IEEE Trans. Antennas Propag.*, Vol. 62, No. 8, 4392–4395, Aug. 2014.
8. Zheng, D.-Z. and Q.-X. Chu, “A multimode wideband  $\pm 45^\circ$  dual-polarized antenna with embedded loops,” *IEEE Antennas Wireless Propag. Lett.*, Vol. 16, 633–636, Jul. 2017.
9. Chu, Q. X., D. L. Wen, and Y. Luo, “A broadband  $\pm 45^\circ$  dual-polarized antenna with Y-shaped feeding lines,” *IEEE Trans. Antennas Propag.*, Vol. 63, No. 2, 483–490, Feb. 2015.
10. Ngytn, D. T., D. H. Lee, and H. C. Park, “Very compact printed triple band-notched UWB antenna with quarter-wavelength slots,” *IEEE Antennas Wireless Propag. Lett.*, No. 11, 411–414, 2012.
11. Seo, Y. S., J. W. Jung, H. J. Lee, et al., “Design of trapezoid monopole antenna with band-notched performance for UWB,” *IET Electronics Letters*, Vol. 48, No. 12, 673–674, 2012.
12. Chen, B., W. Leng, A. G. Wang, et al., “Compact ultra-wideband antenna with reconfigurable notched bands,” *IET Electronics Letters*, Vol. 48, No. 19, 1175–1176, 2012.
13. Liao, X. J., H. C. Yang, N. Han, et al., “Aperture UWB antenna with triple band-notched characteristics,” *IET Electronics Letters*, Vol. 47, No. 2, 77–79, 2011.
14. Yazdi, M. and N. Komjani, “Design of a band-notched UWB monopole antenna by means of an EBG structure,” *IEEE Antennas Wireless Propag. Lett.*, Vol. 10, 170–173, 2011.
15. Hong, J.-S. and M. J. Lancaster, *Microstrip Filters for RF/Microwave Applications*, Wiley, New York, NY, USA, 2001.
16. Gomez-Calero, C., B. Taha Ahmed, and R. Martinez, “A novel ultrawide band frequency planar notch-filter antenna,” *Microw. Opt. Technol. Lett.*, Vol. 52, No. 1, 213–216, Jan. 2010.
17. Zhai, H., J. Zhang, Y. Zang, Q. Gao, and C. Liang, “An LTE base-station magnetoelectric dipole antenna with anti-interference characteristics and its MIMO system Application,” *IEEE Antennas Wireless Propag. Lett.*, Vol. 14, 906–909, 2015.
18. Huang, H., Y. Liu, and S. Gong, “A broadband dual-polarized base station antenna with anti-interference capability,” *IEEE Antennas and Wireless Propag. Lett.*, Vol. 16, 613–616, 2017.
19. Ding, C. F., X. Y. Zhang, Y. Zhang, Y. M. Pan, and Q. Xue, “Compact broadband dual-polarized filtering dipole antenna with high selectivity for base-station applications,” *IEEE Trans. Antennas Propag.*, Vol. 66, No. 11, 5747–5756, Nov. 2018.
20. Kraus, J. D. and R. J. Marhefkas, *Antennas: For All Applications*, 165–196, 3rd Edition, McGraw-Hill, Tempe, AZ, USA, 2002.